

Improved Characterisation of Brain Anisotropy using Diffusion MRI

Marta Correia, Guy Williams, Sally Harding, Thomas Carpenter

Wolfson Brain Imaging Centre, University of Cambridge

Abstract Second order diffusion tensor analysis of diffusion weighted MR data only accounts for a single intra voxel fibre direction. This poses a problem in many regions of the brain where fibres cross. An anisotropy measurement based on the traditional diffusion tensor model, such as fractional anisotropy (FA), produces significantly low values when there are fibres crossing within the same voxel, or in the presence of other partial volume effects. A new anisotropy index based on the variance of the diffusion MRI signal is described and applied to both simulated and experimental data. A method to normalise this parameter, in order to allow comparisons across scan sessions, is also presented. It is shown that this parameter can characterise white matter in situations in which the diffusion tensor formalism fails to accurately reflect the local diffusion. The images obtained show more detail in the fibre structure, a better contrast between regions of high and low anisotropy, and the main fibre tracts appear to be thicker and brighter, which corresponds better anatomically to the information obtained from structural images.

I. INTRODUCTION

Diffusion Weighted Magnetic Resonance Imaging (DWMRI) measures diffusivity in tissues and can provide unique biologically and clinically relevant information that is not available from other imaging modalities. This information includes parameters that help characterise tissue composition, the physical properties of tissue constituents, tissue microstructure, and its architectural organisation. Moreover, these measurements are performed non-invasively and without exogenous contrast agents.

It is well established that the information provided by Diffusion MRI can be very useful in characterising the anisotropy of the brain. However, an anisotropy measurement based on the traditional diffusion tensor model [1], such as fractional anisotropy (FA) [2], produces significantly low values when there are fibres crossing within the same voxel. This observation led to a recent interest in finding alternative measurements of anisotropy, for example, SDV (Spherical Signal Variance) [3] and GA (Generalised Anisotropy) [4]. Here we

describe an anisotropy index based on the variance of the diffusion MRI signal

II. THEORY

When diffusion is isotropic, the MRI signal measured with gradient directions defined on a spherical surface and expressed as the radius from the origin as a function of the spherical coordinates (θ, ϕ) has the shape of a perfect sphere. Anisotropic diffusion deviates from this spherical surface in a manner that depends on the characteristics of the local diffusion (Figure 1). The deviation of the measured signal from the spherical shape can therefore be used as a measure of anisotropy. A way to quantify that deviation is to calculate the MR signal variance:

$$SSV = \langle S^2 \rangle - \langle S \rangle^2 = \frac{1}{N} \sum_{i=1}^N S_i^2 - \left(\frac{1}{N} \sum_{i=1}^N S_i \right)^2 \quad (1)$$

where N is the number of gradient directions used and S_i is the measured MR signal for each direction. We will call this parameter Spherical Signal Variance (SSV). This method allows the identification of regions of diffusion anisotropy in the brain, and avoids the problem of fitting an inappropriate model to the data.

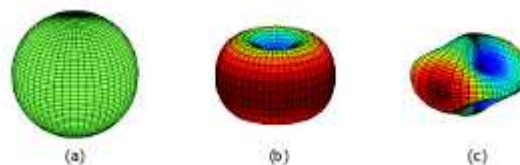


Fig. 1. Spherical coordinates plot of the MR signal of (a) an isotropic voxel, (b) a single fiber and (c) two fibers crossing within the same voxel.

However, the range of values that this index can take is unclear. Typically, an anisotropy index will give a value between 0 and 1, with 0 corresponding to a fully isotropic medium and 1 to an infinitely anisotropic medium. But since SSV is a variance, this index can (in theory) assume any value between 0 and ∞ . $SSV=0$ would still

correspond to perfect isotropy, but the upper limit is not well defined, which makes it difficult to scale the images in a consistent way that allows comparisons between different subjects.

A way to normalise SSV is to use a function defined in the interval $x \geq 0$ and that takes values in $0 \leq f(x) \leq 1$. In addition, this function must be monotonic increasing $x_1 > x_2 \Leftrightarrow f(x_1) > f(x_2)$. The functions that satisfy these two conditions can be divided in two classes:

- functions of type (a) - functions that have non-zero derivative about $x = 0$ ($f'(0) \neq 0$)
- functions of type (b) - functions that have zero derivative about $x = 0$ ($f'(0) = 0$)

Functions of type (a) will tend rapidly to zero as $x \rightarrow 0$, while functions of type (b) will tend to zero slowly. Functions of type (b) will therefore return values very close to zero for low values of x - this will work as a “cut-off” that can be useful to mask even better the noise outside the brain in SSV images. However, this “cut-off” might also mask regions of low anisotropy inside the brain, resulting in a loss on structure detail.

An example of a function of type (a) is:

$$f_a(x) = \tanh(\sigma x) = \frac{e^{\sigma x} - e^{-\sigma x}}{e^{\sigma x} + e^{-\sigma x}} \quad (2)$$

where σ is an adjustable parameter that determines the shape of this function, and a simple function of type (b) is given by:

$$f_b(x) = e^{-\sigma/x^2} \quad (3)$$

A related issue is the comparability of SSV across scan sessions. The use of such a normalisation function does not itself address this problem - in order to do so we must relate SSV to some metric which is repeatable between sessions. This may be done by using the FA map for the same dataset: by selecting some white matter regions of the brain where FA gives comparable values across different subjects we will determine the appropriate value of σ for each dataset.

III. METHODS

A. Comparison between SSV and other anisotropy indices

SSV was calculated for 4 datasets of healthy volunteers carried out at the Wolfson Brain Imaging Centre (WBIC), using a Bruker MedSpec S300 3T scanner. Scans were carried out with the approval of the local ethics committee. A 63 direction encoding scheme [5] with a b-value of 1000s/mm² was used. Diffusion weighting was achieved using a Stejskal-Tanner sequence [7], with pulse width $\delta = 27.5$ ms, inter-pulse spacing $\Delta = 40$ ms TE=85ms and TR=6000ms. The in plane field of view was 20cm (matrix

size 100×100, reconstructed to 128×128) and the slice thickness was 2.0mm. 63 slices were acquired contiguously, with a total scan time of 12 minutes. For comparative purposes, FA, SDV [3] and GA [4] were also calculated. To better compare SSV and FA, simulations were performed for four fibres with different values of anisotropy. Each simulated fiber was first aligned with the gradient frame of reference to give a diagonal tensor \mathbf{D} :

$$\mathbf{D} = \begin{bmatrix} \lambda_1 & 0 & 0 \\ 0 & \lambda_2 & 0 \\ 0 & 0 & \lambda_3 \end{bmatrix} \times 10^{-3} \text{mm}^2 / \text{s} \quad (4)$$

The noise-free diffusion weighted signals were calculated according to the diffusion tensor model [1], assuming an ideal value of the baseline signal $S_0 = 100$. Complex Gaussian noise was then superimposed upon the ideal signals to provide the complex noise-contaminated signals. The noise values were obtained using the routine *gasdev* [6], and scaled so that the signal to noise ratio (SNR), defined as $(\text{ideal } S_0) / (\text{standard deviation of noise})$, could be set to any desired level. A series of SNR were considered in the range of 10-100. The six independent elements of \mathbf{D} and the baseline signal S_0 were fitted simultaneously to all the generated signals using a non-linear least-squares fitting routine [6] to the traditional single tensor model [1]. To evaluate the robustness of the results in the presence of noise, the procedure noise generation \rightarrow creation of noisy data \rightarrow fitting \rightarrow determination of FA and SSV was repeated 2^{13} times, and the mean values and standard deviations were calculated. In addition, variable fibre orientation was realised by spatially rotating the simulated fibres at discrete orientations. 121 orientations were used, which spanned uniformly the space of (θ, ϕ) , $0^\circ \leq \theta \leq 180^\circ$ and $0^\circ \leq \phi \leq 360^\circ$.

B. Normalisation of SSV

To determine the appropriate value of σ in either case, we used the FA map for the same dataset. We first applied a brain extracting tool (BET) to the FA map using FSL 3.3. Then, we selected all the brain voxels in the middle slice of each dataset, and used them to find the value of σ that fits better to $\text{FA} = f_a(\text{SSV})$ and, separately, to $\text{FA} = f_b(\text{SSV})$. The middle slice contains a large quantity of white matter, and it is the slice where the corpus callosum is better defined.

We applied this method to the four datasets used in section III. The selected voxels were fitted to $f_a(x)$ or $f_b(x)$ using optimised non-linear fitting routines for each function. The fitting process associated with $f_b(x)$ is more simple and faster, since we can simply apply a linear least-squares fitting process to $\log(\text{FA}) = -\sigma / \text{SSV}^2$, and use the result as a good initial guess to initialise the non-linear least-squares fit. In the case of $f_a(x)$, finding a good initial estimate is not straightforward, and therefore we used a

Markov Chain Monte Carlo algorithm [8] to find the appropriate value of σ .

IV. RESULTS

A. Comparison between SSV and other anisotropy indices

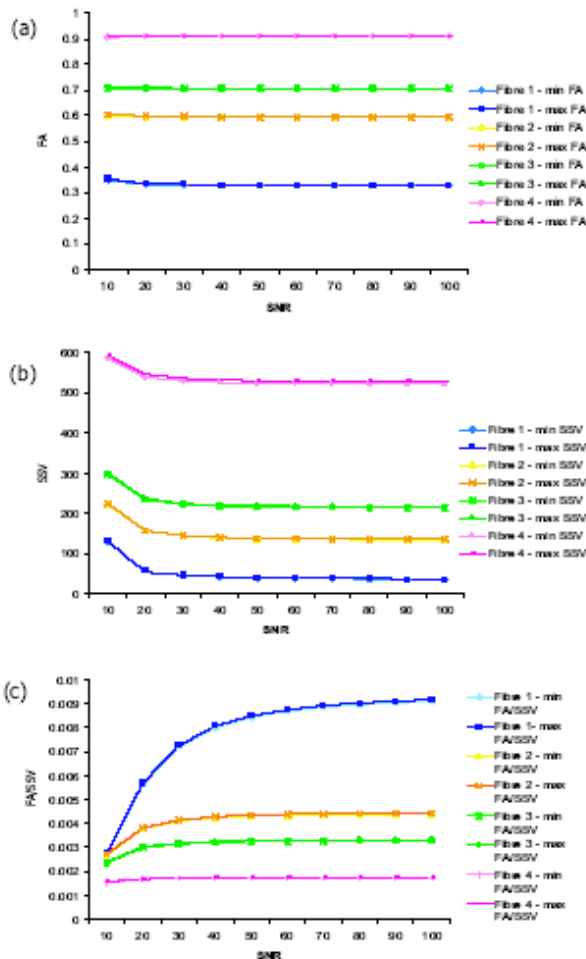


Fig. 2. Results obtained with simulated Fibres 1-4 for: (a) FA, (b) SSV and (c) FA/SSV ratio.

Figure 2 shows the results obtained for FA (Fig 2 (a)) and SSV (Fig 2 (b)) for the simulated Fibres 1-4. For each type of fibre, the ratio between FA and SSV was also calculated, and the results obtained are presented in Figure 2(c).

Figure 2 (b) shows that the higher the simulated anisotropy the higher is the value obtained for SSV, which confirms that SSV can be used as a measurement of anisotropy. However, this image also highlights one of the limitations of using the spherical signal variance as an anisotropy index: the minimum and maximum values of SSV do not converge to the same value as SNR increases, which means that SSV is not rotationally invariant.

The ratio FA/SSV increases as SNR increases, which suggests that FA is more affected by the presence of noise. This could be related to the fact that FA is rotationally independent in the absence of noise and so its performance

improves as we increase the value of SNR. On the other hand, the ratio FA/SSV decreases as the simulated FA increases, which indicates that SSV is more sensitive for high anisotropy regions and will show a higher contrast than FA between regions of high and low anisotropy.

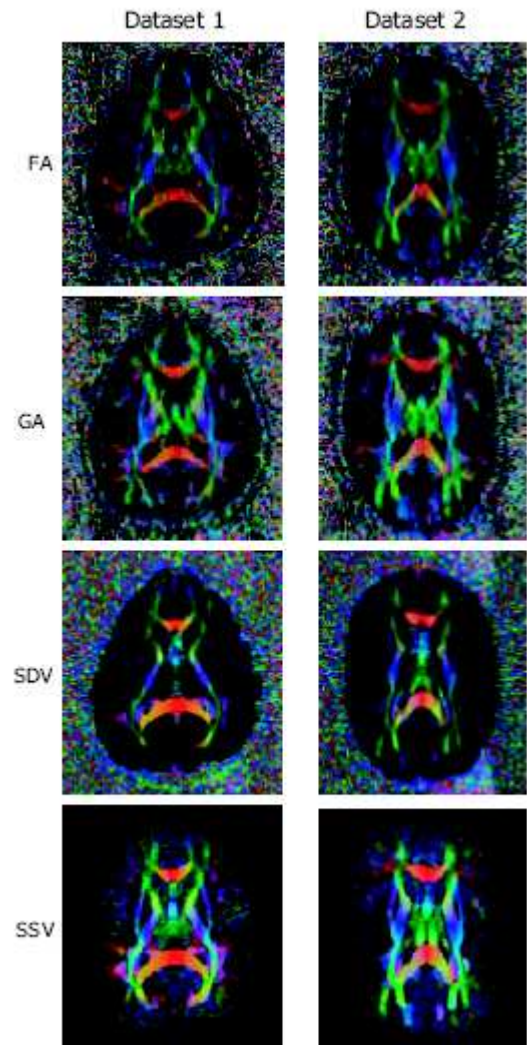


Fig. 3. Orientation colour display maps modulated by FA, GA, SDV and SSV obtained for two of the datasets analysed.

Figure 3 shows the orientation colour display maps modulated by FA, GA, SDV and SSV¹, for the middle slice of two of the four datasets analysed. The images were obtained with FSL View (part of FSL 3.3). When compared to FA maps, SSV images show better contrast between regions of high and low anisotropy, as predicted by the simulations performed. GA images show a better contrast when compared to FA maps, but we can see more detail in the fibre structure in SSV images. It is possible to identify the same structures in FA, GA and SSV maps, but in SSV images the fibre tracts appear to be thicker and

¹ In these color display maps the red, green and blue channels correspond to dx , dy and dz multiplied by an anisotropy index. $d = (dx, dy, dz)$ is the fibre direction estimated by the diffusion tensor model at each voxel.

brighter, which agrees better with the information we get from structural images, especially in the region of the corpus callosum. In addition, the noise outside the brain is automatically cleared in SSV images. This is due to the fact that the variance of the noise is much smaller than the signal variance within the brain. In SDV images the contrast is generally worse and much structure detail is lost. This might be due to the logarithmic scaling necessary to estimate the apparent diffusivity for each voxel, which can introduce additional errors, especially at low values of SNR.

B. Normalisation of SSV

Figure 4 shows the original SSV image compared with the images obtained after normalisation with $f_a(x)$ and $f_b(x)$. Both normalised images and the un-normalised SSV images look very similar: they show the same structures with identical contrasts. However, while it is difficult to identify any differences between SSV and $f_a(x)$ images, the $f_b(x)$ images look slightly more blurry than the original ones, and there is a clear loss of structure detail in the regions of low anisotropy (outside the main fibre tracts). This suggests that a function of type (a) is more suitable for this normalisation process. Table I shows the average values of FA, SSV and normalised SSV (using $f_a(x)$), obtained for a region of interest drawn on the corpus callosum of each analysed dataset. These results confirm that the described normalisation process does produce SSV values comparable across different subjects.

V. DISCUSSION AND CONCLUSION

The local structure of diffusion in voxels with multidirectional fibres can be quite complicated, and it is not necessarily well characterised by a single diffusion tensor. The results obtained with SSV show that this method can characterise white matter in situations in which the diffusion tensor formalism may oversimplify the local diffusion characteristics.

Dataset	FA	SSV	Normalised SSV
1	0.682	0.945	17933.134
2	0.787	0.912	19391.043
3	0.884	0.977	59509.087
4	0.886	0.916	79457.869

TABLE I: AVERAGE VALUES OF FA, SSV AND NORMALISED SSV OBTAINED FOR A REGION OF INTEREST DRAWN ON THE CORPUS CALLOSUM OF EACH ANALYSED DATASET.

Even though the results obtained with SSV show a general improvement when compared to FA results, this technique has two important limitations. First, SSV is not rotationally invariant. This means that two voxels with the same degree of anisotropy but different orientations could show up with completely different contrasts in an SSV map. However, this limitation is not exclusive to SSV: in

the presence of noise the estimated FA depends on the fibre orientation (as do all the traditional anisotropy indices), and for signal to noise ratios around 10 (the values of SNR we typically obtain with experimental data) the relative variation $((\max-\min)/\max)$ of FA is similar to the relative variation of SSV. Secondly, the range of values that this index can take is unclear, which makes it difficult to scale the images in a consistent way that allows comparisons between different subjects. This issue was addressed in sections III-C and IV-C and it has been shown that SSV images can be normalised without any significant loss of detail in fibre structure. The results obtained with two different normalisation functions were compared. In both cases, the main fibre tracts appear very well defined, but some structure detail is lost in the regions of low anisotropy when we use a function of type (b). This is most probably due to the “cut-off” effect described earlier and illustrated in Figure 10. For this reason, even though the fitting process associated with $f_b(x)$ is faster, the results obtained by this process are worse than the ones obtained with $f_a(x)$. Future work will include the application of this method to datasets acquired from patients, in order to assess how this parameter changes in pathological conditions.

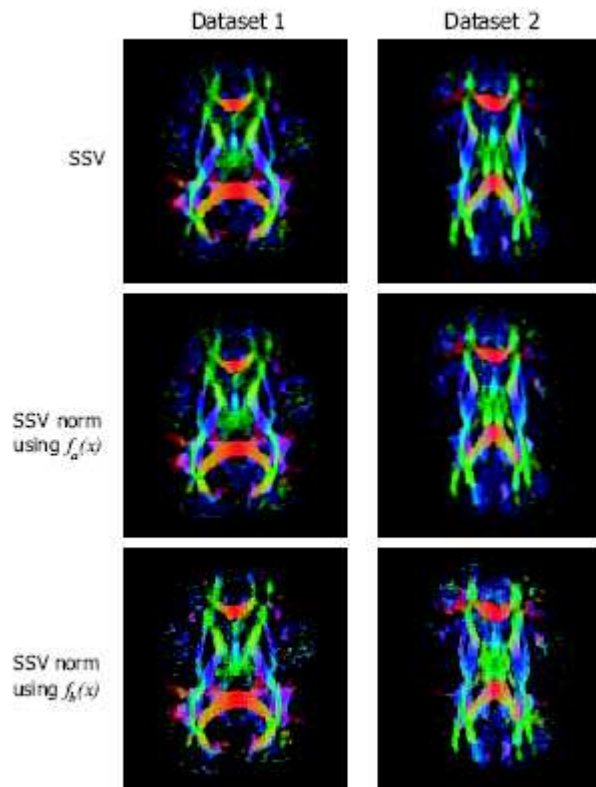


Fig. 4. SSV images for datasets 1 and 2 compared with the images obtained after normalisation with $f_a(x)$ and $f_b(x)$.

REFERENCES

- [1] Bassar PJ, Mattiello J, LeBihan D. Estimation of the effective selfdiffusion tensor from the NMR spin echo. *J Magn Reson, Series B* 103: 247-254, 1994.
- [2] Bassar PJ, Pierpaoli C. Microstructural and physiological features of tissues elucidated by quantitative diffusion tensor MRI. *J Magn Reson Series B* 111: 209-219, 1996.
- [3] Frank LR. Anisotropy in high angular resolution diffusion-weighted MRI. *Magn Reson Med* 45: 935-939, 2001.
- [4] Ozarslan E, Vemuri BC, Mareci TH. Generalised Scalar Measures for Diffusion MRI Using TRace, Variance and Entropy. *Magn Reson Med* 53: 866-876, 2005.
- [5] Hardin RH, Sloane NJA, Smith WD. Minimal energy arrangements of points on a sphere. <http://www.research.att.com/njas/electrons/dim3/>.
- [6] Press WH, Vetterling WT, Teukolsky SA, Flannery BP. *Numerical Recipes in C (Second Edition)*. Cambridge University Press, 2002.
- [7] Stejskal EO, Tanner JE. Spin Diffusion Measurements: spin echoes in the presence of time dependent field gradients. *J Chem Phys*, 42: 299, 1965.
- [8] Gilks W, Richardson S, Spiegelhalter D. *Markov Chain Monte Carlo in Practice*. Chapman and Hall/CRC, 1996.